한국기계가공학회지, 제19권, 제10호, pp. 16～23(2020.10) ISSN 1598-6721(Print)
Journal of the Korean Society of Manufacturing Process Engineers, Vol. 19, No. 10, pp. 16~23(2020.10) ISSN 2288-0771(Online)

https://doi.org/10.14775/ksmpe.2020.19.10.016

Durability Analysis of Automotive Seat According to the Shape of Seat Back Frame

Kyekwang Choi*, Jaeung Cho**,#

*Department of Metal Mold Design Engineering, Kongju National UNIV.,
**Division of Mechanical and Automotive Engineering, Kongju National UNIV.

시트백 프레임의 형상에 따른 자동차 시트의 내구성 해석에 관한 연구

최계광*, 조재웅**,#

*공주대학교 금형설계공학과, **공주대학교 기계자동차공학부

(Received 20 February 2020; received in revised form 18 March 2020; accepted 19 March 2020)

ABSTRACT

Vehicle seats provide a comfortable ride for passengers by properly absorbing vibrations and shocks transmitted during driving. Vibration analyses on three models with different shapes were carried with the same material properties and constraint conditions. By varying the height of the seat-back, models 1, 2, and 3 were designed according to the inclined angle of the seat-back frame. Models 1, 2, and 3 were modeled with relatively simple designs using CATIA. The areas touching the buttocks of passengers show the most deformation. This work shows that seat durability and stability can vary depending on the shape of the seat design.

Key Words : Seat Back Frame(시트백 프레임), Shape(형상), Durability(내구성), Equivalent Stress(등가 응력), Natural Frequency(고유 진동수)

1. Introduction

With the development of human-centered design and manufacturing technologies in the automotive industry, reduction in vehicle vibration and noise has rapidly improved. As a result, the automotive features positioned nearest customers are important to customers buying their own vehicles. Thus, many automotive companies have worked toward evaluating and improving seat capabilities in a variety of ways[1-4]. In a vehicle seat, the vibration due to the state of the road surface directly influences passenger comfort. The seat frame also serves to protect passengers in a collision[1-3]. Recently, high-efficiency, eco-friendly automobiles have been developed in order to comply with stricter environmental regulations. However, the weight is inevitably increased in order to increase

Corresponding Author : jucho@kongju.ac.kr
Tel: +82-41-521-9271, Fax:+82-41-555-9123

vehicle performance, which has been a major concern from the early stages of vehicle development. Improving vehicle performance and reducing fuel consumption results in higher design costs. Many safety regulations must be satisfied by vehicle seats. The vehicle seat consists of the head restraint, the back frame, the cushion frame, and the seat support for passenger safety. Vibration analyses on three models with different shapes were carried out with the same material properties and constraint conditions[5-8]. Models 1, 2, and 3 were modeled with relatively simple designs by using CATIA. The areas touching the buttocks of passengers show the most deformation. This work shows that seat durability[9-10] and stability can vary by depending on the shape of the seat.

2. Study Models and Boundary Conditions

2.1 Study Models

In this study, the rear seat frame of the car was modeled to reflect reality. Three models designed using the CATIA program are shown in Fig. 1. Models 1, 2, and 3 are fixed to the rails at the base of the seat, and model 3 has a greater bending angle than the other models. The material properties of aluminum alloy, as used in the models, are shown in Table 1. The numbers of nodes and elements on each model are shown in Table 2.

2.2 Constraint Conditions

Models 1, 2, and 3 were designed according to the inclined angle of the seat-back frame by varying the height. All analyses were carried out using the ANSYS program. Constraint conditions for a running vehicle are as follows: a load of 30000 N in the Z+ direction, a force from the wheel in contact with the ground. Fig. 2 shows the fixed supports and loading directions for each model[9-10].

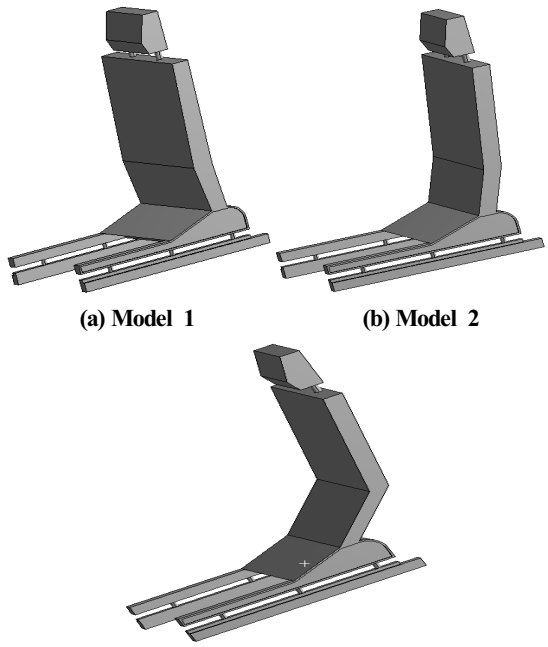

(a) Model 1 (b) Model 2

(c) Model 3

Fig. 1 Analysis models

Table 1 Material properties of models

Intents	Values
Compressive yield strength	250 MPa
Poisson's ratio	0.3
Young's modules	2×10^5 MPa
Tensile ultimate strength	460 MPa
Density	7850 kg/m^3
Tensile yield strength	250 MPa

Table 2 Numbers of elements and nodes on models

Model	Nodes	Elements
Model 1	51980	32230
Model 2	50016	30760
Model 3	50630	30949

3. Result

3.1 Structural Analysis

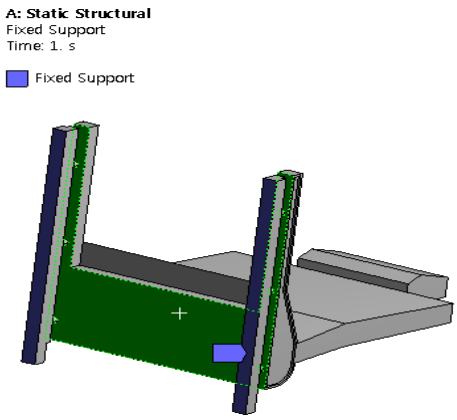

(a) Fixed support at model 1

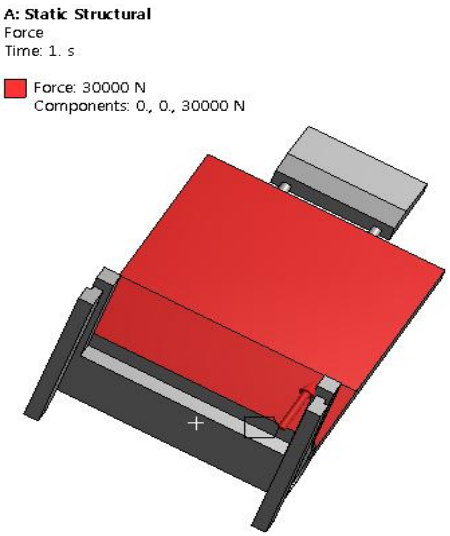

(b) Loading condition at model 1

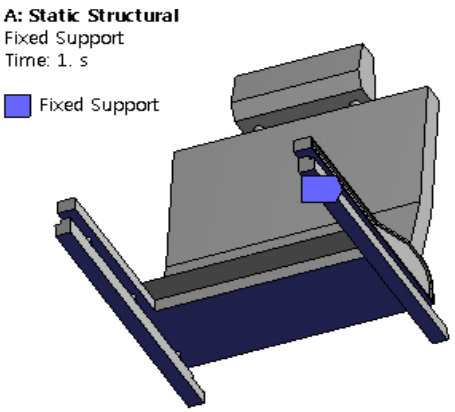

(c) Fixed support at model 2

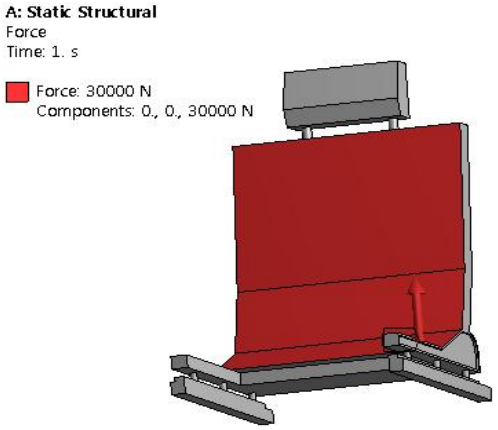

(d) Loading condition at model 2

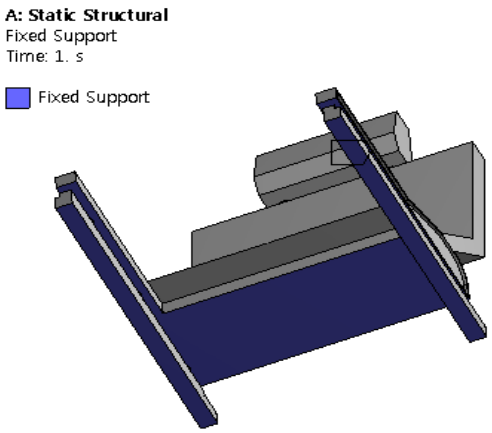

(e) Fixed support at model 3

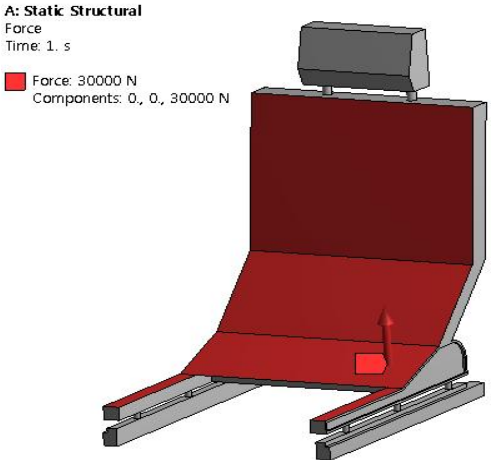

(f) Loading condition at model 3

Fig. 2 Constraint conditions for each model

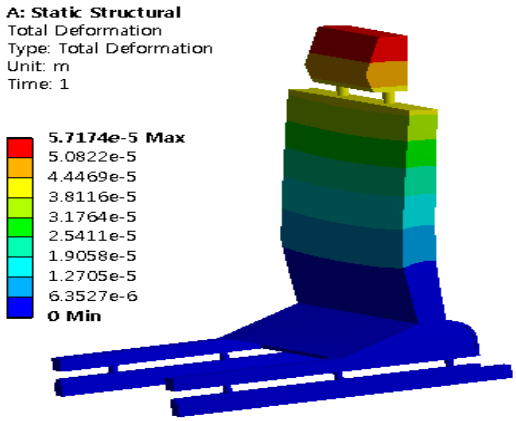

(a) Model 1

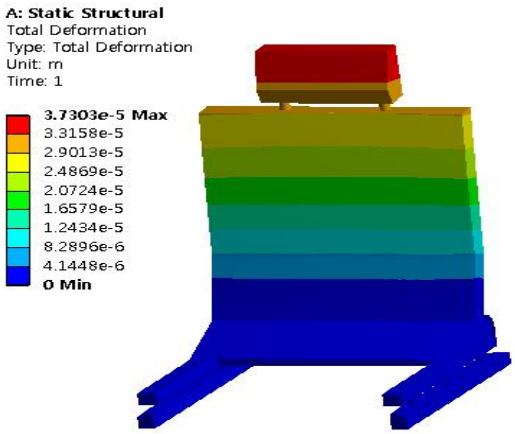

(b) Model 2

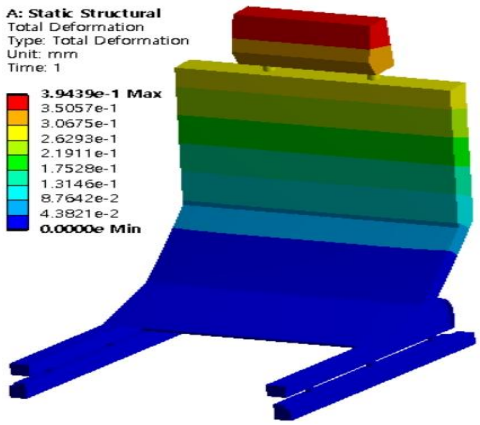

(c) Model 3

Fig. 3 Contours of total deformations at structural analysis

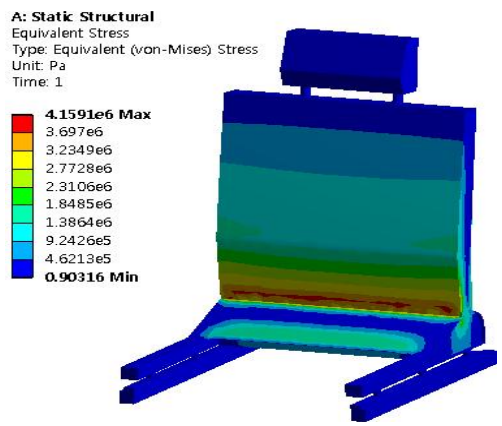

(a) Model 1

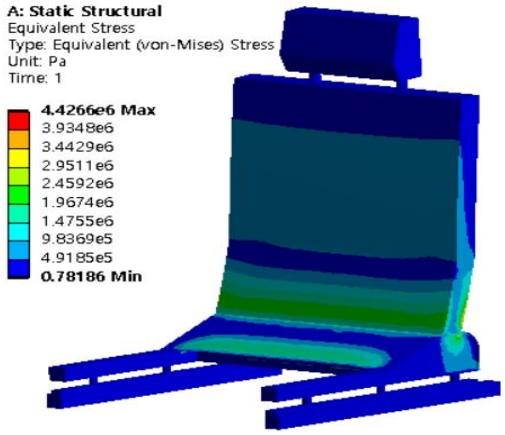

(b) Model 2

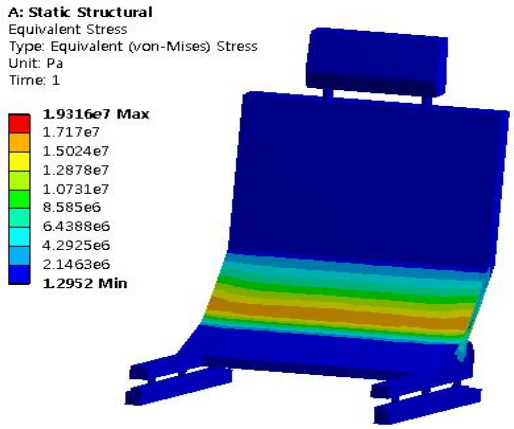

(c) Model 3

Fig. 4 Contours of equivalent stresses at structural analysis

Figs. 3 and 4 show the contours of total deformations and equivalent stresses for each model. Assuming that a load of 30000 N was acting from the underside of the vehicle, the maximum deformations shown in Fig. 3 are 0.0057174 mm, 0.0037303 mm, and 0.39439 mm for models 1, 2, and 3, respectively. The maximum equivalent stresses shown by Fig. 4 are 4.1591 MPa, 4.4266 MPa and 19.316 MPa for models 1, 2, and 3, respectively. Among all models, model 1 exhibits the highest structural strength, while model 3 exhibits the lowest structural strength.

3.2 Vibration Analysis

In order to examine the natural frequency of the automotive seat, vibration analyses were carried out by applying a fixed support condition, as shown in Fig. 2. Tables 3, 4, and 5 show the maximum total deformations on the natural frequencies at modes 1, 2, 3, 4, 5, and 6 for each model. All models exhibit maximum total deformation at mode 6. Models 1, 2, and 3 have maximum deformations of 39.938 mm, 37.154 mm, and 34.661 mm, respectively. At the same time, the maximum natural frequencies vary from 800 Hz to 900 Hz for models 1, 2, and 3. Models 1, 2, and 3 have minimum natural frequencies of 96.92 Hz mm, 86.406 Hz mm, and 60.196 Hz, respectively. Vibrations due to natural frequencies occur below 1000 Hz for all models. Fig. 5 shows the amplitude stress which occurs in the harmonic vibration range from 0 Hz to 1000 Hz. Further, the peak amplitude stresses show the critical states for each model. At the maximum stress amplitude, models 1, 2, and 3 have critical frequencies of 870 Hz, 790 Hz, and 60 Hz, respectively.

Figs. 6 and 7 show the contours of total deformations and equivalent stresses at the critical frequencies at models 1, 2, and 3. Models 1, 2, and 3 exhibit maximum total deformations of 0.046694 mm, 0.048122 mm and 7.7858 mm, respectively.

Table 3 Maximum total deformations on natural frequencies by mode in case of model 1

	Natural frequency(Hz)	Maximum total deformation(mm)
1'st mode	96.92	32.496
2'nd mode	204.86	26.796
3'rd mode	381.79	25.603
4'th mode	587.87	25.83
5'th mode	869.21	24.444
6'th mode	892.37	39.938

Table 4 Maximum total deformations on natural frequencies by mode in case of model 2

	Natural frequency(Hz)	Maximum total deformation(mm)
1'st mode	86.406	29.936
2'nd mode	188.55	30.232
3'rd mode	320.04	25.187
4'th mode	589.2	24.052
5'th mode	785.81	22.039
6'th mode	826.94	37.154

Table 5 Maximum total deformations on natural frequencies by mode in case of model 3

	Natural frequency(Hz)	Maximum total deformation(mm)
1'st mode	60.196	23.433
2'nd mode	159.48	35.292
3'rd mode	201.44	19.335
4'th mode	481.41	25.077
5'th mode	534.94	16.95
6'th mode	818.68	34.661

Models 1, 2, and 3 have maximum equivalent stresses of 56.18 MPa, 58.601 MPa, and 789.3 MPa, respectively. Among the three models, model 1 exhibits the strongest vibration durability, while, model 3 exhibits the weakest vibration durability.

4. Conclusion

In this study, structural and vibration analyses on three vehicle seat models with different shapes were

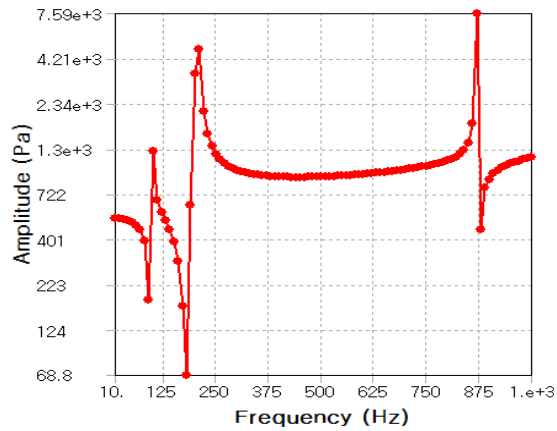

(a) Model 1

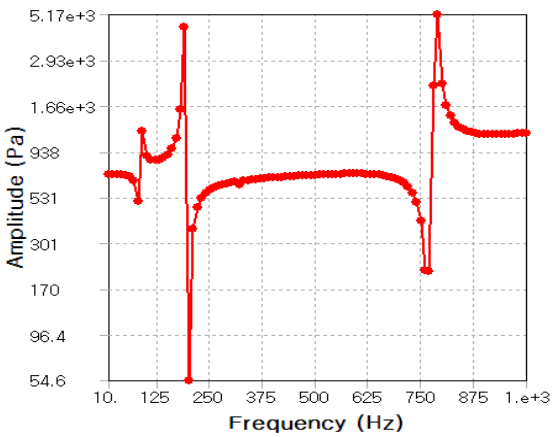

(b) Model 2

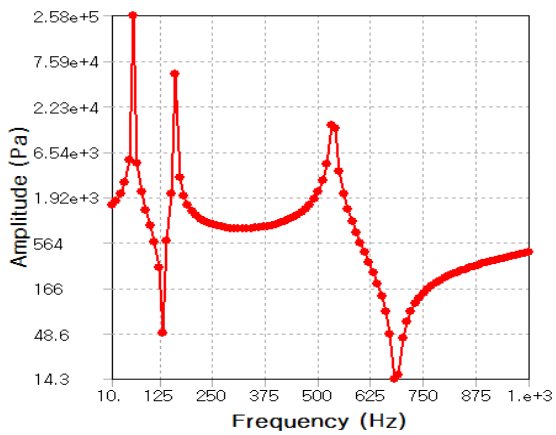

(c) Model 3

Fig. 5 Frequency responses of amplitude stresses at models 1, 2 and 3

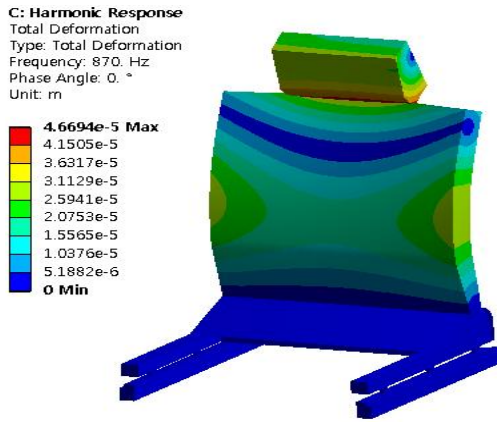

(a) Model 1

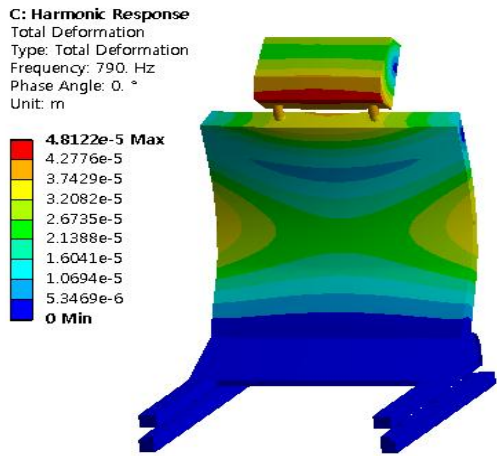

(b) Model 2

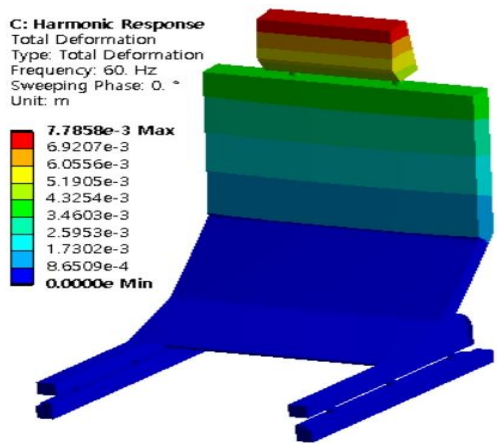

(c) Model 3

Fig. 6 Total deformations at critical frequencies

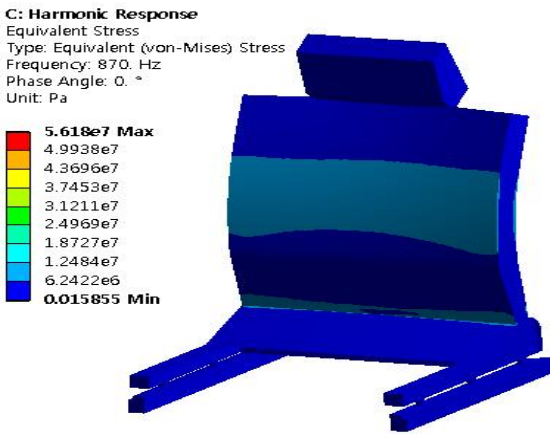

(a) Model 1

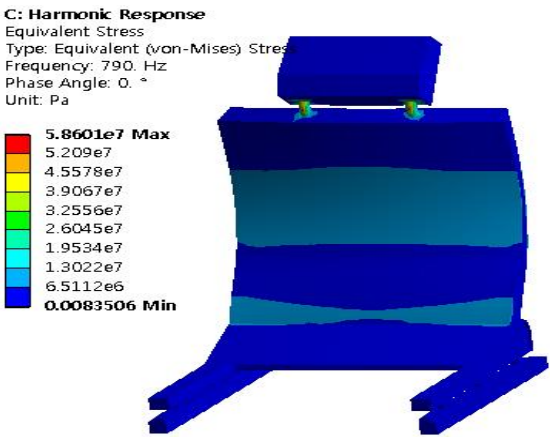

(b) Model 2

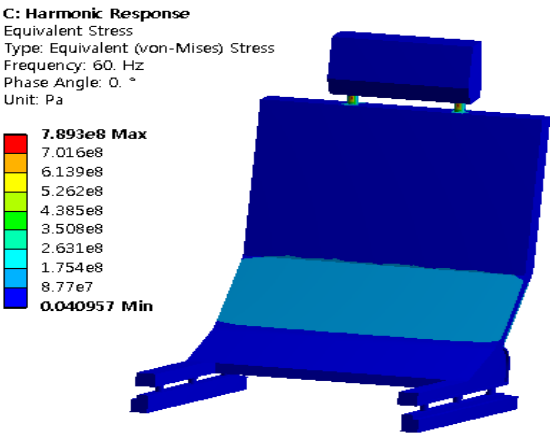

(c) Model 3

Fig. 7 Equivalent stresses at critical frequencies

carried out. The results are summarized as follows:

1. Among all models, model 1 exhibits the highest structural strength, while model 3 exhibits the lowest structural strength.
2. The maximum natural frequencies range from 800 Hz to 900 Hz for models 1, 2, and 3.
3. With a structural force of 3000 N, harmonic vibration occurred on the seat frame. Among all models, model 1 exhibits the strongest vibration durability, while model 3 exhibits the weakest vibration durability.
4. The durability and stability of the automotive seat frame vary depending on the shape of the seat.

REFERENCES

1. Oh, Y. T., “Study on the Structural Analysis of SCARA Industrial Robot,” Journal of the Korean Society of Mechanical Technology, Vol. 19, No. 6, pp. 866-871, 2017.

2. Lee, Y. S. and Yand, Y. Y., “Study on Structural Analysis of Variable Roll Unit for Drawing Process of SUS Hexagonal Bar,” Journal of the Korean Society of Mechanical Technology, Vol. 19, No. 6, pp. 827-833, 2017.

3. Lee, D. H. and Cho, J. U., “Convergence Study on Damage of the Bonded Part at TDCB Structure with the Laminate Angle Manufactured with CFRP,” Journal of the Korea Convergence Society, Vol. 9, No. 12, pp. 175-180, 2018.

4. Park, J. W., “Structural Analysis of a Tractor Cabin Considering Structure Production Error,” Journal of the Korea Convergence Society, Vol. 8, No. 5, pp. 155-160, 2017.

5. Ko, J. H. and Kang, D. M., “CAE Analysis on Strength and Fatigue of Rear Door of Passenger Car,” Journal of the Korean Society of

Manufacturing Process Engineers, Vol. 13, No. 3, pp. 63-69, 2014.
6. Ha, S. H., Kim, S. J. and Song, J. I., “Structure Analysis and Torque Reduction Design of Industrial Ball Valve,” Journal of the Korean Society of Manufacturing Process Engineers, Vol. 13, No. 6, pp. 37-45, 2014.
7. Choo, S. W. and Jeong, S. H., “Structural and Dynamic Characteristic Analysis of a Feeder for an Automatic Assembly System of an LED Convergent Lighting Module,” Journal of the Korean Society of Manufacturing Process Engineers, Vol. 16, No. 1, pp. 124-133, 2017.
8. Kang, H. J., Kim, B. H., Kim, B. H. and Seo, J. H., “Structural Weld Strength Analysis on Door Hinge of Field Artillery Ammunition Support Vehicle,” Journal of the Korean Society of Manufacturing Process Engineers, Vol. 15, No. 3, pp. 58-65, 2016.
9. Lee, S. E., Lee, T. W. and Kang, Y. G., “Shock Analysis of Gimbal Structure System Including Rubber Vibration Isolator in a Observation Reconnaissance Aircraft,” Journal of the Korean Society of Manufacturing Process Engineers, Vol. 13, No. 2, pp. 73-80, 2014.
10. Son, I. S., Kim, C. H., Bae, S. H. and Lee, J. Y., “Rescue Lift Development Using Structural Analysis,” Journal of the Korean Society of Manufacturing Process Engineers, Vol. 14, No. 1, pp. 111-116, 2015.